Materials Science & Engineering A 724 (2018) 189–198

Contents lists available at ScienceDirect

Materials Science & Engineering A

journal homepage: www.elsevier.com/locate/msea

Observations on {332} < 113 > twinning-induced softening in Ti-Nb Gum metal

Sumin Shin[a], Chaoyi Zhu[a], Kenneth S. Vecchio[a,b,*]

[a] Materials Science & Engineering Program, University of California, La Jolla, San Diego, CA 92093-0448, United States
[b] Department of NanoEngineering, University of California, La Jolla, San Diego, CA 92093-0448, United States

ARTICLE INFO

Keywords:
Metastable titanium alloy
Gum metal
EBSD
Deformation twining
Schmid factor

ABSTRACT

Thermomechanical-cycling processes were applied to a metastable Ti-23Nb-0.7Ta-2Zr-1.0O (at%) alloy to control a volume fraction of mechanical twins, resulting from activation of twinning-induced plasticity effects. Analysis of the microstructure features designed using electron backscattering and X-ray diffraction revealed the deformation bands induced by the cycling process were characterized as only {332} < 113 >$_{\beta}$ twinning. It was also observed that the fraction of twins was significantly increased with increasing the number of the cycles in the process, resulting in a pronounced softening effect. To shed a light on the relevant micro-scale features (e.g., geometric orientation and stress concentrations) responsible for the microstructure evolution and mechanical response, the local Schmid factor of grains and geometrically-necessary dislocation densities were evaluated from experimentally observed results, and correlated with deformation twinning. A good correlation between the local geometric Schmid factor and softening behavior, due to texture evolution within twins was established, as well as the effect of local stress concentrations on microstructure evolution of this Ti-Nb Gum metal. Significant decrease in micro-hardness (approximately 18% from untwinned structure) was achieved by highly twinned structure, and a possible deformation mechanism was established to enhance ductility without evident elastic properties variation in metastable β Ti alloys.

1. Introduction

Recently, the development of metastable β-titanium alloys, which can be defined as the least stable β-phase Ti alloys, are known to possess a good combination of extremely low elastic modulus and a high specific strength [1]. These alloys have been widely considered to be utilized as promising biomaterials in artificial hip and knee joints, etc. to reduce the stress shield, which is caused by high Young's modulus of the implant, compared with that of human bone (max. 30 GPa) [2,3]. In recent years, several new β alloys such as TNS (Ti–25Nb–11Sn (wt%)) [4], Ti-2448 (Ti-24Nb-4Zr-8Sn (wt%)) [5] and TNTZ (Ti-29Nb-13Ta-4.6Zr (wt%)) [2,6] have been developed for applications as metallic structure implants as well as a replacement for hard tissue [4–7]. However, due to the relatively poor formability compared to other conventional alloys, their translation into commercial applications has been hindered. As a result, further investigations have been undertaken to open new possibilities to expand the material property window between the relatively low Young's modulus, which is related to chemical composition optimization [1] and better formability [8,9], which is linked to improved ductility and enhanced strain hardening [8–11]. With progress in improving formability, a prominent approach has been considered to stimulate activation of multiple deformation modes, such as mechanical twinning or stress-induced transformation, along with dislocation slip, and thus significantly improve upon the poor ductility caused by rapid strain localization in slip-dominated β-Ti alloys [10,11]. However, it is difficult to separately manipulate the mechanical properties of these alloys, without affecting the Young's modulus variation (avoiding increasing the modulus), which is the most prominent property of these metastable β-Ti alloys for consideration in biomaterial implants.

For example, Gum metals, which fundamentally consist of Ti-Nb-Ta-Zr elements, along with intentional amounts of oxygen, have been developed by optimized alloy design for “super-properties” such as low elastic modulus (50–90 GPa), very high strength (~1.1 GPa) and superelasticity (~2.5%) [11–17]. Owing to its unique physical properties and good biocompatibility, Gum metals are expected to be potential biomedical materials. However, this alloy development effort has not focused on improved plastic deformation behaviors related to higher ductility and better formability. As an example, the oxygen introduced in the Gum metal chemical composition may help retard athermal

* Corresponding author at: Department of NanoEngineering, University of California, La Jolla, San Diego, CA 92093-0448, United States.
E-mail address: kvecchio@eng.ucsd.edu (K.S. Vecchio).

https://doi.org/10.1016/j.msea.2018.03.062
Received 4 January 2018; Received in revised form 13 March 2018; Accepted 14 March 2018
Available online 21 March 2018
0921-5093/

α″-martensite and ω-phase transformations, which are beneficial to achieve its unique elastic properties [13,14], whereas ductility and formability of Gum metal are significantly decreased by the addition of oxygen, which is mainly due not only to oxygen solute strengthening [15], but also suppression of the deformation twinning mechanism by increasing β-phase stability [16].

Twining is an important deformation mode in several metastable β-Ti alloys, and it is well documented in the literature that the origin of {332} < 113 > twinning strongly depends on crystallographic orientation [17,18], which was substantiated based on Schmid's law. In addition, Marteleur et al. [10] reported that deformation twining plays a crucial role in exhibiting a large uniform elongation and significant straining hardening, as evident from Twinning-Induced Plasticity (TWIP) steels [19–21]. Although the improvement in these mechanical properties has not yet been fully understood or utilized, the activation of multiple {332} < 113 > twinning is an essential key to enhance formability in metastable Ti alloys [10,18,22]. It is worth noting that, whereas the occurrence of mechanical twining in these alloys has been extensively studied, twin fraction/mechanical property relationships have received little attention and not optimized due to a lack of experimental information on highly twinned structures of β-Ti alloys.

As a consequence, this study was focused to achieve multiple twinning in a Ti-23Nb-2Zr-0.7Ta-1.0O (at%) alloy, attributed to an optimized microstructure design approach. Significant decrease in hardness without evident Young's modulus variation was achieved through the formation of highly twinned structure, and a possible deformation mechanism was discussed. To understand the microstructure evolution during plastic deformation, stress concentrations were estimated qualitatively with geometrically-necessary dislocation (GND) densities derived from electron backscattered diffraction (EBSD) measurements. In addition, different fractions of twins were employed to elucidate the relevant microstructure features responsible for the variation in mechanical properties, based on the global Schmid factor analysis. Therefore, the main objective of this study was to understand the effect of microstructure features on deformation evolution and the mechanical properties in the Ti-Nb Gum metal resulting from extensive plastic deformation processing.

2. Experimental procedures

2.1. Twinned structure design

In order to achieve twinning-induced microstructural features, a unique cycling process (CP) composed of a small pre-strain step and subsequent heat treatment was adopted in this study. A fully homogenized Gum metal alloy was first cold-rolled to 5% reduction ($\varepsilon = 0.05$) leading to the formation of the primary deformation twins, attributed to the presence of different crystallography orientation within the parent grain and lattice distortions caused by local stress concentrations. This pre-strain level provided a sufficient trigger stress for the nucleation of the primary twin bands in the grains, and neither the secondary bands, generally formed into the primary band, nor significant the primary band growth were found with the 5% reduction. Next, a heat treatment step was carried out at 973 K for 30 min, with sufficient time at temperature to relieve local stress concentrations adjacent to the deformation bands and grain boundaries, but still avoid detwinning of the deformation twins by recrystallization and/or boundary migration. The presence of athermal martensitic phases can lead to undesired properties, such as embrittlement and increases in Young's modulus [1,23]. Therefore, a rapid water cooling step was selected to maintain a homogenized structure, which is beneficial to suppress growth of recrystallized grains and limit precipitation of athermal ω and/or α″ martensitic phases. The process was implemented as a sequence of up to four cold-rolling/heating/cooling cycles able to achieve varying twin fractions in the microstructure of the Gum metal. These thermomechanical-cycling processed specimens are referred to hereafter as CP1, CP2, CP3 and CP4, respectively.

Table 1
Chemical composition of as-cast Ti-Nb-Ta-Zr-O alloy.

Element	Ti	Nb	Ta	Zr	O
at%	Balance	22.8	0.72	2.05	1.0
wt%	Balance	35.5	2.18	3.13	0.27

2.2. Experimental details

Gum metal with a nominal chemical composition of Ti-23Nb-2.0Zr-0.7Ta-1.0O (at%) was prepared by arc-melting under argon atmosphere, with a mixture of pure elements Ti, Nb, Ta, Zr, and TiO_2. For the preparation of fully homogenized specimens, the ingots were held in an inert-gas induction furnace for 30-min in its liquid state, then solution-treated for 2000-min at 1273 K (above the β transus), followed by water quenching [24]. The measured chemical composition of the as-cast alloy is presented in Table 1. It is shown that the microstructure of the as-solution treated alloy consists of random oriented grains with an average size of ~650 μm (Fig. 1a). Phase identification was conducted by X-ray diffraction (XRD) using Cu-Kα radiation. The body-centered cubic β-phase was the only phase detected in the alloy as shown in Fig. 1b. For these experiments, all samples were subjected to mechanical polishing with SiC papers and SiO_2 solutions under a load of 5 N. Microstructure observations of the polished surfaces were carried out via optical microscopy (OM) and electron backscatter diffraction (EBSD) on the cross-section parallel to the rolling-direction (RD) using a Bruker e-Flash EBSD detector on a FEI Quanta 600 SEM at 20 kV. To investigate the effect of deformation twinning on the mechanical and elastic properties, as well as establish the dependence of these properties on the cycling process, micro-hardness and elastic modulus measurements were conducted using Vickers hardness and acoustic wave method, respectively. The experimental methods and conditions for these mechanical tests were described in our previous work [24].

2.3. Schmid factor and GND

To further explore the orientation information, Schmid factor (SF) and geometrically necessary dislocation (GND) densities were analyzed using EBSD results. Data were collected from four distinct 38 μm × 50 μm scans at different locations on the same cross section of samples. Based on orientation of parent grains and {332} < 113 > twin variants, it was possible to obtain Schmid factor values using the available Bruker EBSD software. The Schmid factor presented in this study is the global Schmid factor, which ignores the complex internal stress state variation [25]. It is calculated for every pixel of the EBSD image in the following manner. First, the orientation matrix is used to rotate individual twin variants from crystal coordinates to sample coordinates. Next, the global Schmid factor of individual twin variants in the sample coordinates can be calculated as a product of the direction cosines between the loading direction and individual twinning direction/plane. GND density is calculated based on measured orientation data from Hough-based EBSD through the Nye tensor, while ignoring the relatively insignificant elastic strain gradients. From the orientation descriptor, i.e. Euler angles, lattice misorientation matrices can be extracted from pairs of neighboring pixels, which are used for computing lattice orientation gradients to populate the Nye tensor [26]. A traction free boundary condition is reasonably assumed for the interrogated surface material, therefore only five terms of the Nye tensor are directly accessible from the measured data (α_{12}, α_{13}, α_{21}, α_{23}, α_{33}), plus an extra difference term (α_{11}-α_{22}) [27]. Through Frank's loop construction, the measured Nye tensor can be equated with the unknown dislocation density vector and the dislocation configuration matrix formed by dyadics of the Burgers vectors and

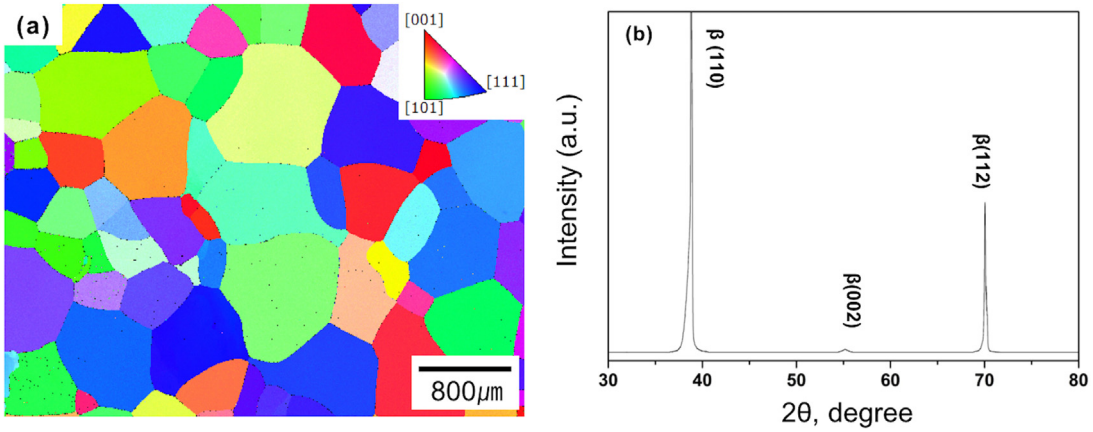

Fig. 1. (a) Microstructure and (b) XRD patter of the solution-treated alloy.

unit line directions. Erroneous GND density data points are then filtered out, including those below the noise floor and those adjacent to sub-grain or grain boundaries. In this study, the dislocation density statistics are generated through log-normal probability density function fitting of the data distribution [28].

3. Results

3.1. Mechanical properties

Fig. 2 shows the variation of microhardness and Young's modulus with increasing the number of cycling process (CP) steps compared to those of specimens subjected to cold-rolling reductions (CR) to 5%, 15% and 20%, corresponding to the same amount of thickness reduction with CP1, CP2 and CP4, respectively. Young's modulus measurements reveal that there was little or no difference in the specimens subjected to the cycling process versus cold-rolling alone to 15%. On the other hand, Young's modulus with cold-rolling to 20% reduction decreased slightly from 78 GPa to 69 GPa, which was beneficial for cold-worked Gum metal [11]. For mechanical properties, typical process methods or deformation mechanisms that accumulation of strain are associated with an increase in hardness and strength of polycrystalline, a phenomenon commonly known as work hardening behavior. This was observed in the Gum metal with cold-rolling reduction to 20%, although with a relatively low work-hardening rate, based on the hardness measurement shown in Fig. 2, as compared to conventional β-Ti alloys, which is attributed to non-conventional dislocation-free deformation mechanisms [11,29,30]. However, the Gum metal samples subjected to the thermomechanical-cycling process exhibit a different hardness trend compared to the cold-rolled specimens. The data reveal that micro-hardness significantly decreased with increasing number of CP steps, with approximately 20% decrease in hardness even with a thickness reduction to 20% from the solution-treated alloy. These results appear to be in conflict with the dynamic Hall-Petch mechanism for strengthening by deformation twinning as previously described in the literature [19–21,28], since twin boundaries are generally considered to be obstacles to dislocation-based plasticity. The present study is thus focused particularly on this softening behavior induced by the cyclic processing, and establish and validate the mechanism associated with this softening effect depicted in Fig. 2.

3.2. Phase constitution

Fig. 3 shows XRD results of the 20% cold-rolled Gum metal and thermomechanical-cycling processed Gum metal. Only the peaks related to the body centered cubic (bcc) β-phase were indexed in the Gum metal after 20% reduction (20CR in Fig. 3), implying that cold deformation has no obvious influence on phase constitution of the single phase β microstructure. However, evidence for the C-centered orthorhombic α″ martensitic formation was found in CP-Gum metals, as indicated in Fig. 3. This demonstrates the occurrence of thermally-induced martensitic transformation β → α″ during heat treatment, which

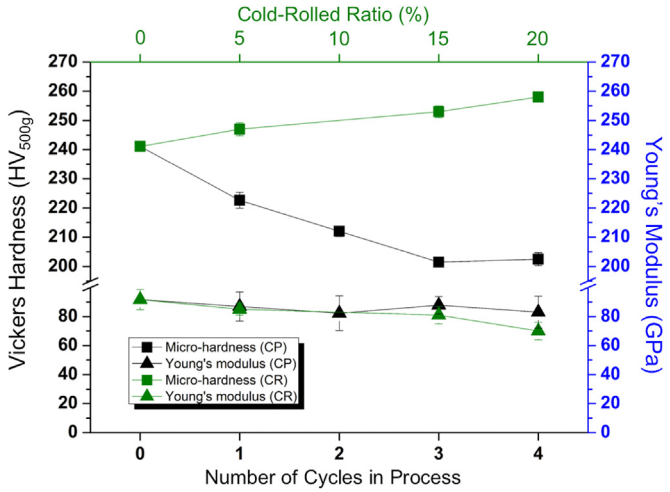

Fig. 2. Variations of microhardness and Young's modulus with the number of cycling process and cold-rolled ratio.

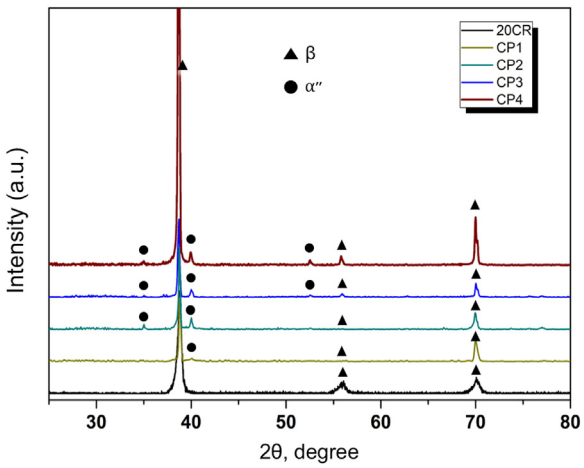

Fig. 3. XRD patterns of Ti-Nb-Ta-Zr-O alloys subject to 20% cold rolling and the thermomechanical-cycling process from one to four cycles (CP1, CP2, CP3 and CP4).

was mainly attributed to a lower process temperature (923 K) than β-transus temperature, as it has been reported earlier for numerous metastable β Ti alloys [31–34]. Comparing the intensity of α″ phase peaks among the samples, the highest intensity and more evident α″ peaks were observed in CP4 specimen. This suggests a higher volume fraction of α″ phase in the CP4, which may be correlated to the enhancement of the thermally-induced martensitic transformation by increased total heat treatment time with each cycle. It is worth noting that constituent phases of the alloy are closely linked to Young's modulus and hardness of metastable β-Ti alloys [24], and it has been observed previously that β-phase microstructure possesses a lower hardness and Young's modulus compare to those of α″ phase-dominated structures [35–37]. Based on the results as depicted in Fig. 2, however, the amount of α″ phase formed during the CP had a negligible effect on mechanical and elastic properties of the processed Gum metal in this study. In addition, it has been reported previously that the precipitation of isothermal martensitic phases in β-phase dominated Ti alloys, such as ω- and/or α″-phase, would significantly influence its deformation mechanism, which is mainly dependent on β-phase stability [38,39]. From the microstructure observations (it will be shown in Section 3.3), it can be seen that plastic deformation induced by the thermomechanical process was mainly attributed to mechanical twinning, irrespective of phase constitution. This also supports the conclusion that neither deformation mechanism in Gum metal nor β-phase stability would be influenced by the precipitation of isothermal α″ phase.

3.3. Microstructure

To compare the microstructures between cold-rolled specimens and the thermomechanical-cycling processed specimens, EBSD analysis was carried out. The microstructures in the Gum metal samples exhibit significantly different features between these two processes after the as-solution treated state. Fig. 4a and b show the representative microstructures of the specimens after cold-rolling to 5% ($\varepsilon = 0.05$) and 20% ($\varepsilon = 0.2$) reduction, respectively. The color code was used for grain orientation in all IPF maps is given in the upper right corner of Fig. 4a. In the deformed Gum metal, at 5% reduction, a few deformation bands, tens of micrometers in size, were observed with different fractions in each grain, shown in Fig. 4a. In addition, crystallographic orientations identified in the elongated deformation bands differ from that of the β-parent phase, caused by twinning deformation. This implies that a lattice reorientation of the twinned regions would make it change the condition of plastic deformation, based on geometric factors. The crystallographic orientation obtained from EBSD analysis will be discussed in the Section 4 to interpret the deformation behavior in Gum metal. In our previous work [24], mechanical {332} < 113 > β twinning was preferred as the active deformation mechanism, especially at the early stages of cold deformation, suggesting that the deformation bands formed during the cold rolling process are mainly consistent with {332} < 113 > β twins induced by plastic deformation. The microstructure features shown in Fig. 4b show that the fraction of deformation bands identified as {332} < 113 > β twins was unchanged with increasing reduction from 5% to 20%, although strain localization was observed in a few grains, which is in good agreement with the typical deformation behavior of Ti-Nb Gum metal [11,14,15]. This implies that plastic deformation with further cold rolling proceeds mainly through the activation of other mechanisms, such as dislocation slip, kinking, and shear band formation, resulting in significant strain hardening [16] when compared to twinning-dominated plastic deformation. Conversely, in the specimens that were processed by a combination of pre-strain and subsequent heat treatment (CP samples) shown in Fig. 4c, a large fraction of deformation bands was observed. In the inset of Fig. 4c, which is the enlarged microstructure, several recrystallized grains, with the size of a few micrometers, were also found in the deformation bands, resulting from the combined effects of localized strain in the bands and heat treatment. From the misorientation analysis (along the line inset of Fig. 4c), the plate-like features were confirmed to be typical {332} < 113 > β twins (indicated with blue lines) that corresponds to the crystallographic misorientation of 50.5° between the β-matrix and {332} < 113 > β twin along the < 110 > β direction [17]. The IPF maps shown in Fig. 4 indicate that mechanical twinning was induced by not only pre-strain, but rather enhanced by further deformation in the thermomechanical-cycling process. Furthermore, the obtained results demonstrate that microstructure features in Gum metals were strongly linked to its mechanical properties, especially the softening behavior associated with the twinning, as mentioned in Section 3. A better assessment of the effect of multiple twinning on the mechanical response was achieved using a Schmid factor analysis, which will be discussed in Section 4.

3.4. Microstructure evolution in the thermomechanical-cycling processed Gum metal

To uncover the microstructure evolution in the thermomechanical-cycling processed Gum metal, microstructures corresponding to the CP1 and CP2 were characterized by EBSD analysis, and the results obtained are displayed in Fig. 5. Dramatic changes in the microstructure features were apparent as the number of CP increased. In Fig. 5(a) and (b), the observed microstructure in CP1 shows numerous plate-like bands consisting of {332} < 113 > β twins, which were identified with the misorientation profile shown in Fig. 5c. These bands were introduced by plastic strain to 5% reduction ($\varepsilon = 0.05$) by the first CP, and the width of the primary twins are approximately 10–20 μm determined from the Fig. 5c. It should be noted that the initially induced twins appear to nucleate from one boundary and terminate at another grain boundary. In addition, the majority twin bands formed in the same grain exhibited the same orientation as shown in the IPF map (Fig. 5a), implying that they were formed under the same geometrical deformation condition. The secondary twins were also observed within the primary ones, in which the secondary deformation, formed by the first cold-rolling, was preferred to be active within the primary twin due to the modification of the geometrical orientation in the twinned β zones, as reported earlier [40]. In the microstructure of CP2 shown in Fig. 5(d) and (e), more densely distributed deformation features were observed compared to that of CP1. A few deformation twins appeared to have different orientations from others in the same grain, as seen in the IPF map (Fig. 5d). As seen in Fig. 5e, the number of deformation bands were significantly increased as evident by the abundance of the dark areas which are heavily deformed regions. Further observations reveal that some grains were also deformed sufficiently to have a wavy structure of bands, demonstrating that grain rotation and twisting occurred with further deformation, resulting in new twins as indicated with arrows in Fig. 5d. According to the misorientation analysis shown in Fig. 5f, the occurrence of newly formed deformation bands present in the CP2 were also identified as {332} < 113 > β twins. Furthermore, the new twins with the width of only a few micrometers were mainly introduced in un-deformed β regions of the CP1. The reason for the discrepancy in twin thickness between CP1 and CP2 was considered to be strain localized in the un-deformed β zones during the second CP, which is associated with increasing activation energy for twin nucleation.

In Fig. 6, the representative microstructures of CP3 (a and b) and CP4 (c and d) observed of etched surface with optical microscopy are displayed. Numerous deformed lamella structure as well as several recrystallized grains a few microns in size were observed. It should be noted that these features were observed throughout the specimens, irrespective of location; however, it was not possible to evaluate accurately the number of deformation band and their thickness due to highly deformed structure. Indeed, the variation of bands was found to be increased and more pronounced as the cycling process proceed to CP4. It was also seen in Fig. 6b and d that the fine deformation traces within the twins exhibit consider waviness between the twin bands in

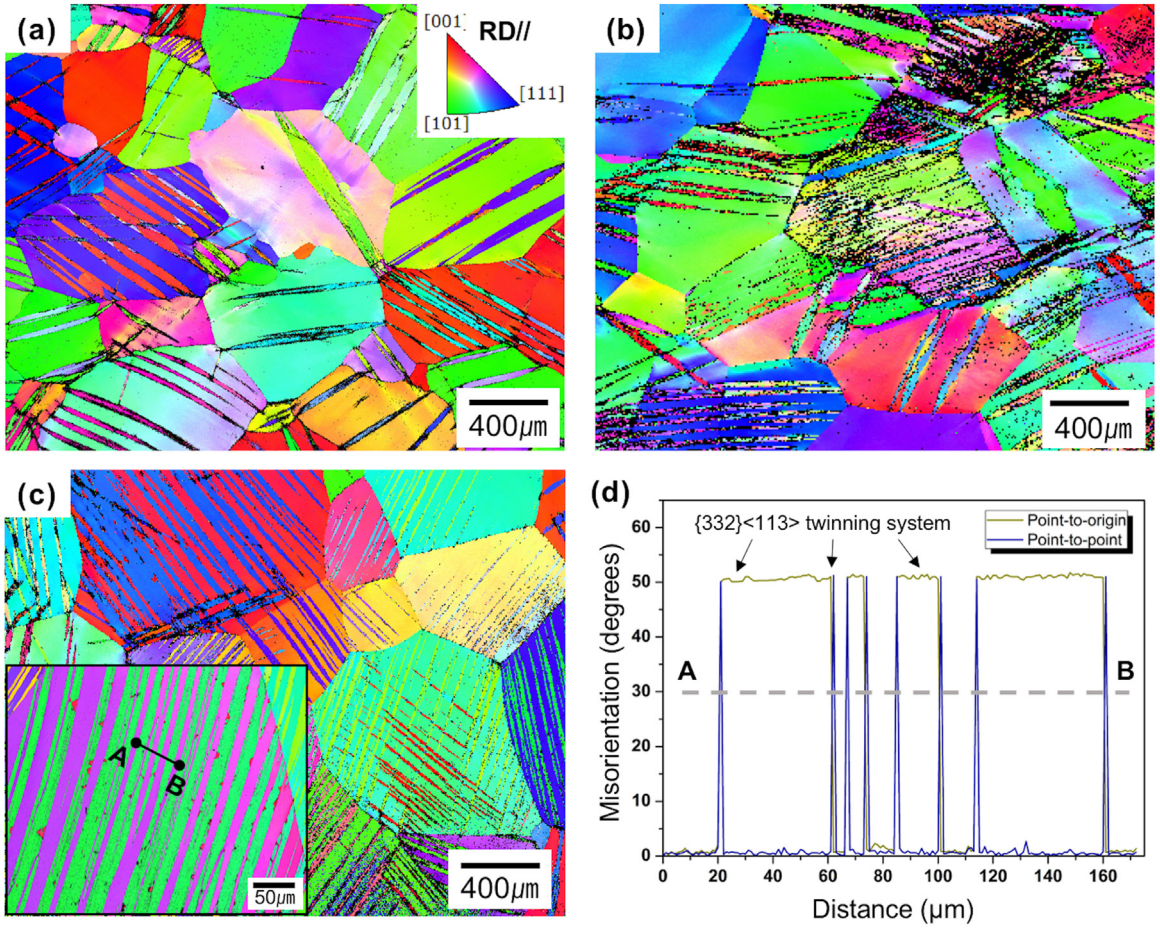

Fig. 4. Inverse pole figure maps showing the deformation microstructures of specimens with a strain of (a) 0.05; (b) 0.2, and (c) microstructure of CP4. (d) Misorientation profile along the along the arrow AB of the inset image in (c).

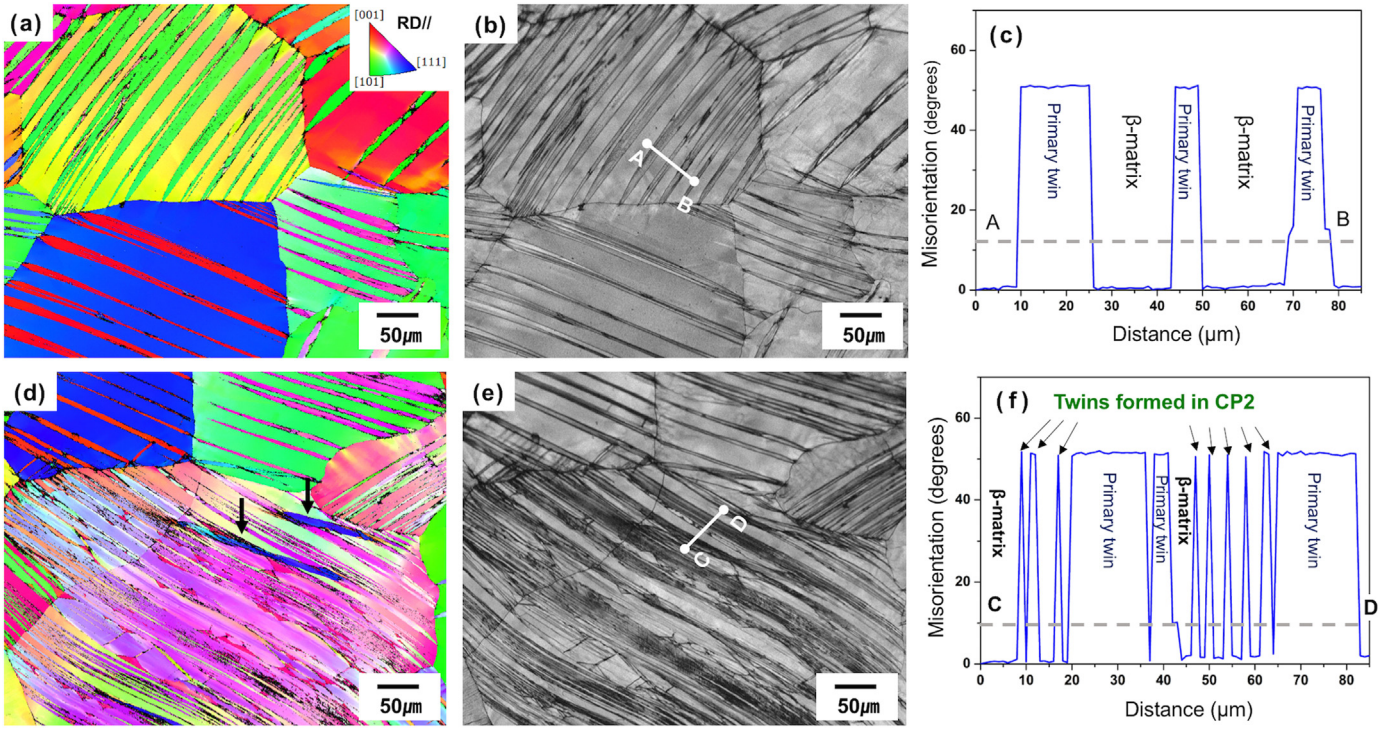

Fig. 5. EBSD results of CP1(a-c) and CP2(d-f): (a), (d) IPF maps, (b), (e) the corresponding IQ maps and (c), (f) misorientation profiles along trace AB in (b) and CD in (e), respectively.

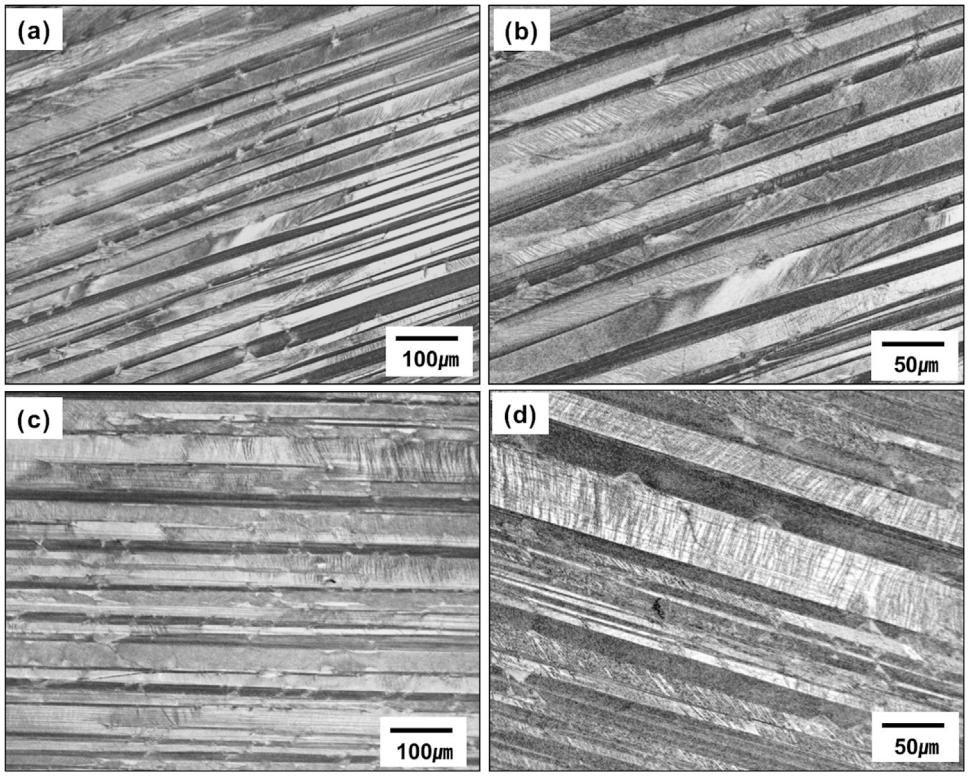

Fig. 6. Optical micrographs showing the microstructures of (a), (b) CP3 and (c), (d) CP4. Micrograph plane is parallel to the rolling direction (RD).

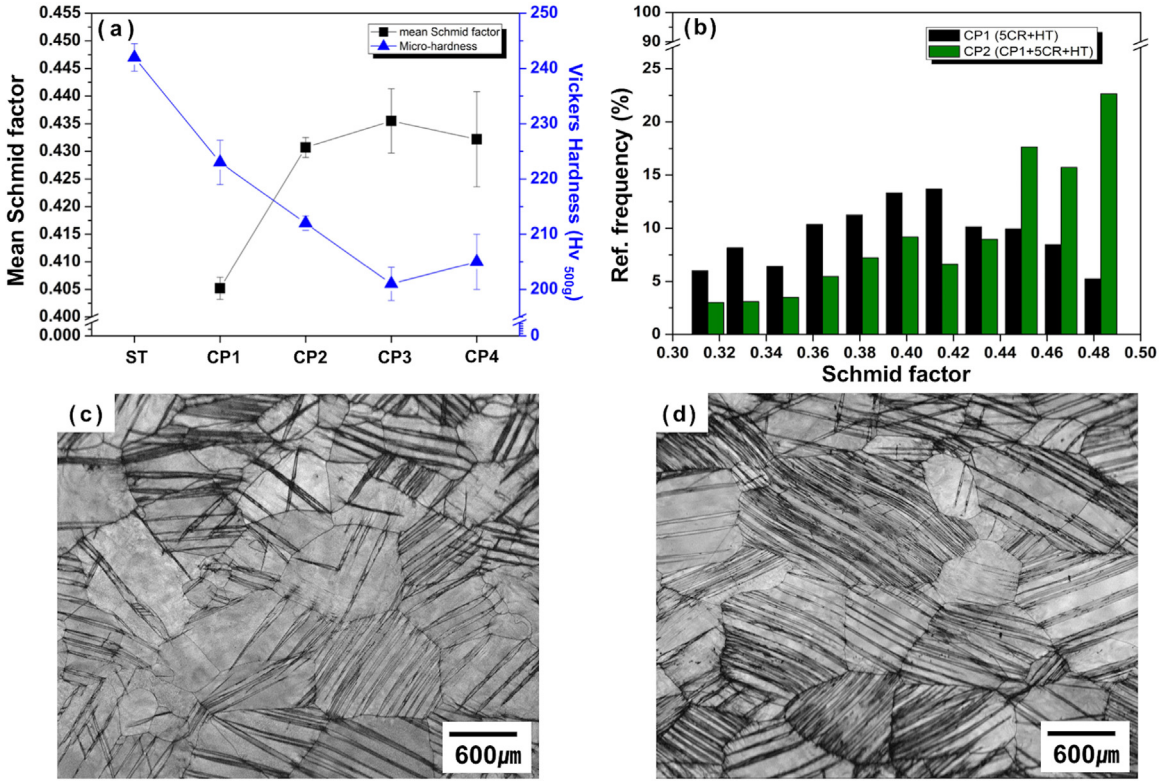

Fig. 7. Deformation twinning dependence of Schmid factor (SF): (a) variations mean Schmid factor and Vickers hardness with the number of CP with the error bars showing the standard deviation, (b) SF distributions of CP1 and CP2, and IQ maps of (c) CP1 and (d) CP2, respectively. Measured surface is parallel to the rolling direction.

the un-deformed zones (indicated as bright area in the observed microstructures), which is a different deformation behavior compared with CP1 and CP2. These results demonstrate that the highly twinned structure induced by the thermomechanical-cycling process was obviously derived from the different deformation condition when compared to when only cold rolling deformation was applied. The

microstructure evolution sequence associated with the thermo-mechanical-cycling process will be discussed further in Section 4.

4. Discussion

4.1. Effect of the geometric Schmid factor on softening behavior

Experimental observations from this study illustrate a highly twinned microstructure in a metastable Ti-Nb Gum metal can be achieved by the thermomechanical-cycling process described herein, composed of repeated cycles of a pre-strain and subsequent heat treatment. In addition to twin-induced plasticity (TWIP) effect, exhibiting low yield strength and large uniform elongation through significant work hardening, which have been reported previously [7-11,18,40-44], it was found that the multiple twins significantly affect microstructure evolution and mechanical response in this study. The trend of decreasing hardness, shown in Fig. 2, in the Gum metal, with increasing twin fraction, can be well explained by softening mechanism in terms of a crystallographic orientation of deforming crystal structure. Earlier reports [38,45–47] suggest that deformation twinning can induce a structural softening in the twinned region, due to texture evolution associated lattice reorientation, as indicated in Fig. 5. The modified orientation in the twinned structure is ascribed to a favorable geometrical condition for the secondary deformation twins. Hence, it implies that the contribution to softening will be significant the larger the fraction of deformation twins in the microstructure.

In order to clarify the effect of orientation-dependent on twinning activation, the Schmid factor (SF) was calculated with EBSD data, considering the resolved external stress on the twinning plane and in the twining shear direction [17]. Combining the hardness results of CP specimens in Fig. 2, with the mean Schmid Factor analysis, reveals that the trend of the measured hardness with the number of CP steps was strongly related with the variation of SF values, as depicted in Fig. 7a. It should be noted that the fine newly formed twins observed throughout the microstructures of CP3 and CP4 (Fig. 6) were not considered as part of the mean SF values due to the inability of the EBSD technique to resolve these features, where thickness of the twins were smaller than the step size (~0.85 μm) used for EBSD analysis or the corresponding interaction volume. Only absolute SF values larger than 0.3 were considered to activate plastic deformation, as reported by Bertrand et al. [17]. During the thermomechanical-cycling process, the average Schmid factor increased mainly due to a larger volume of twinned regions with increasing the number of CP steps. Fig. 7(a) and (b) present the distribution of Schmid factors on the population of observed twins, for the CP1 and CP2 samples respectively. For the CP1 sample, the average SF values increase from 0.403 to 0.429, while for the CP2 samples the values are demonstrably higher with a range from 0.45 to 0.49, close to the maximum value of 0.5. It is noted that more twins were found with higher Schmid factors. In Fig. 7(c) and (d), the representative microstructure in the CP1 and CP2 obtained by EBSD image quality maps reveal that the volume fraction of deformation twin increased as the cycling process proceeded, due to not only pre-strain, which induced the primary twins in the CP1, but also further deformation, which introduced newly formed twins in CP2, as illustrated in Fig. 5. This result demonstrates that the variation of Schmid factor with the number of the CP steps was strongly linked to microstructure features, correlated with the fraction of deformation twins.

Fig. 8 show inverse pole figure (IPF) maps of the CP1 and CP2 with the corresponding Schmid factor (SF) distribution maps, illustrating that reorientation was accompanied by deformation twin. According to the SF maps shown in Fig. 8(b) and (d), the twinned region has a much higher SF value than that of the β-matrix. The results are in agreement with previous literature [41,48] in β-Ti alloys, where the secondary deformation was preferentially activated in the twinned regions

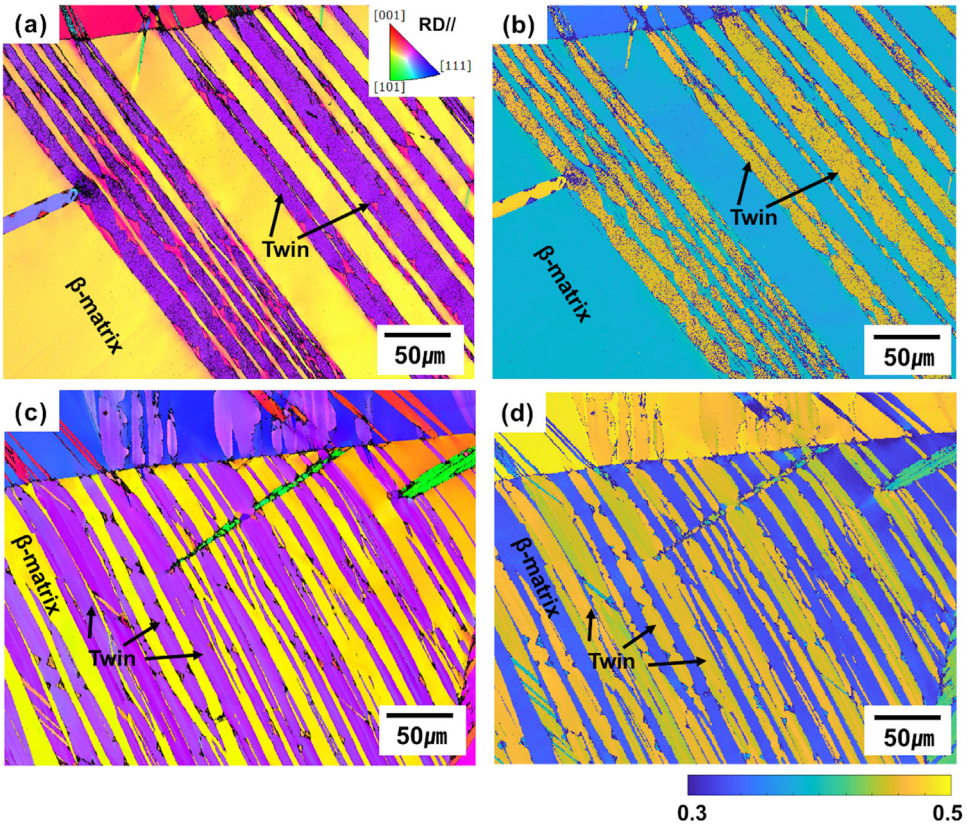

Fig. 8. Twinning structures of (a) CP1 and (c) CP2, and the corresponding Schmid factor distribution maps of (b) CP1 and (d) CP2. The scale indicates the calculated SF value.

because of a modified orientation factor, based on the Schmid factor. This also supports the conclusions that the mechanical softening in Ti-Nb Gum metal is governed by the initial twin fraction in the microstructure, which might be attributed to orientation dependence of the critical resolved shear stress in twin-dominated deformation [17,48–50].

4.2. Effect of local stress concentrations on microstructure evolution

The results in this study lead to a question of why twin formation would be further enhanced in the cyclically processed Gum metal. From Schmid factor analysis, it can be expected that further plastic deformation is likely to be active in twin bands rather than in un-twinned regions. Based on Fig. 5 and Fig. 6, however, the observations demonstrate that the activation of new deformation twins induced by the cyclic process preferentially occurred in the un-twinned regions, implying that the microstructural evolution correlates to a different deformation behavior when compared to that of the cold-rolled Gum metal. Indeed, numerous studies on the nucleation of deformation twin in a polycrystalline material have been suggested non-Schmid factor behavior associated deformation twin formation [51–53]. The postulated non-Schmid factor mechanism has been explained by local stress concentrations. For instance, a twin variant formed in a grain is not always related with the highest Schmid factor, and some of the twins were shown to form in regions of the second highest or even much lower SF values, for example in [17,41,51]. In addition, Guo et al. [25] reported deformation twins can cause a localized stress field at the twin tip and at the interface between the twin and parent grain, which was highly correlated with the lengthening and thickening of the twins by further external stress. This implies that the twining process, including nucleation, propagation and thickening, would be strongly dependent on the localized event (or stress concentration), based on a resolved shear stress that is determined by the stress tensor in the twinning region rather than the Schmid factor alone. To elucidate this point further, the Kernel Average Misorientation (KAM) was analyzed by the EBSD data, which can represent relative strain concentration; misorientations greater than a tolerance of 3° were excluded. Fig. 9 display the IPF maps (a and c) and the corresponding KAM maps (b and d) of the specimen subject to cold-rolling to 15% (a and b), and cyclic processed (CP2) (cold-rolled + annealing). The IPF map shows from the cold-rolled sample (Fig. 9a), the relatively coarse deformation twins, with approximately 50–70 μm wide, represents a thickening dominated phase of the twinning process. The misorientation analysis shown in Fig. 9b demonstrates that a stress concentration was significantly localized at the twin tip and at twin-parent interface, resulting in a very heterogeneous stress distribution. From these results, it can be stated that, with only cold deformation (no annealing step), an external stress applied after the primary twin formation would mainly assist thickening of the twins through local stress concentrations around the twin-parent interface (thickening state) rather than nucleation of new twins. On the order hand, clearly different microstructural features, with a large number of parallel thin twins (see Fig. 9c), were revealed in the cyclically processed specimen, as compared to the twins in Fig. 9a. This implies that nucleation of new twins predominantly occurred in the deformation process rather than thickening of existing twins, which might be attributed to lower strain (and hence stress) concentrations. As depicted in Fig. 9d, the CP2 sample, having undergone annealing before the additional cold-rolling, was identified with almost the same KAM values throughout the whole grain, indicating that the level of stress concentrations from strained (cold-rolled only) state to annealed (CP) state change sharply.

A better assessment of the effect of local stress concentrations on twin formation was achieved by the determination of the density and distribution of geometrically necessary dislocations (GND), which are associated with non-uniformly deformed regions of a material [54]. GND density is calculated based on measured orientation data from Hough-based EBSD through the Nye tensor, while ignoring the relatively insignificant elastic strain gradients. Fig. 10 shows the GND density of strained state (5CR) (by cold rolling to 5%) was higher than that of the annealed state (5CR + annealing) by subsequent heat

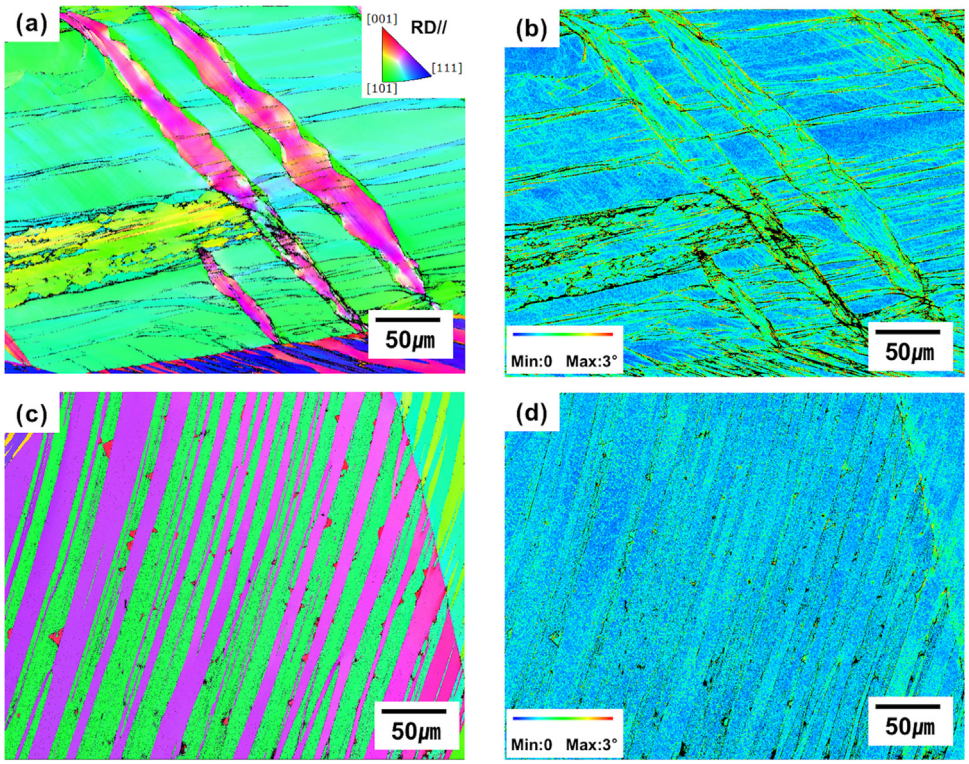

Fig. 9. EBSD analysis of specimen subject to: (a), (b) cold-rolling to 15% and (c), (d)CP2: (a), (c) IPF maps and (b), (d) the corresponding Kernel average misorientation maps. The scale indicates the misorientation value excluding greater than a pre-set tolerance value of 3°.

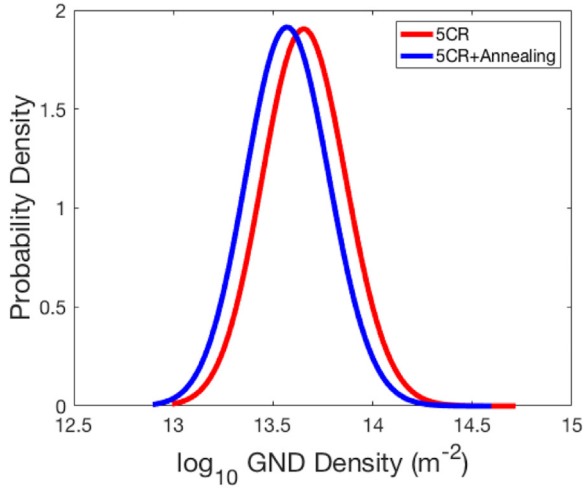

Fig. 10. Comparison of GND density as a function of stress states between strained structure (5CR) and annealed structure (5CR + Annealing) in the Ti-Nb Gum metals.

treatment. The comparison between the two GND densities reveals that the local stress concentration might have been modified slightly by recovery of the distorted lattice after heat treatment (annihilation of dislocations). Accordingly, it demonstrates that small stress gradients, which could drive the nucleation of new twin at grain boundaries, and enhanced local stress concentrations (e.g., at twin tips and grain boundaries), which would be beneficial for twin thickening, were strongly dependent on the microstructure state of the Gum metal. These results lead to a very important conclusion that controlling stress states (particularly dislocation densities and their distributions) is an essential key to achieve the highly twinned structure that contribute to the softening behavior in the mechanical response of Ti-Nb Gum metals.

5. Conclusions

In order to investigate the effect of twin fraction (after being deformed) on mechanical properties in a Ti-23Nb-0.7Ta-2Zr-1.O (at%) alloy, a microstructure design approach was utilized, which incorporated both highly twinned structures and highly strained structures. The geometric Schmid factor and GND density of the resulting microstructures were analyzed following a study of texture softening and microstructure evolution. The main results in this work are summarized as:

1. The goal of a highly twinned microstructure was successfully obtained through the thermomechanical-cycling process by a combination of pre-strain (5% cold-rolling) and subsequent heat treatment (973 K, 30 min), which was mainly composed of {332} < 113 > β twinning.
2. Microhardness measurement revealed that the twinning structure was strongly related to the overall softening behavior, showing that more twins result in lower hardness in the Gum metal. However, Young's modulus was largely unaffected by twin fraction and isothermal α″-phase present in these alloys.
3. The Schmid factor analysis demonstrated that there was structural softening in twinned regions, caused by texture reorientation associated with a more favorable orientation for plastic deformation.
4. Local stress concentrations mainly induced by twin formation plays an important role in determining the deformation evolution of Ti-Nb Gum metal. It was found that reduced localized stress variation (resulting from the annealing step) facilitates the nucleation of new twins at grain boundaries. Whereas, in the cold-rolled condition, propagation and thickening of pre-existing twins were enhanced due to the higher stress concentrations at the twin tips and/or the interface between twins and β-parent phase.

Acknowledgements

The authors would like to thank C. Zhang, T. Harrington, and H. Wang, University of California, San Diego, for their helpful suggestions, stimulating discussions and constant encouragement.

References

[1] D. Banerjee, J.C. Williams, Perspectives on titanium science and technology, Acta Mater. 61 (2013) 844–879.
[2] Q. Li, M. Niinomi, J. Hieda, M. Nakai, K. Cho, Deformation-induced ω phase in modified Ti-29Nb-13Ta-4.6Zr alloy by Cr addition, Acta Biomater. 9 (2013) 8027–8035.
[3] Y. Song, D.S. Xu, R. Yang, D. Li, W.T. Wu, Z.X. Guo, Theoretical study of the effects of alloying elements on the strength and modulus of β-type bio-titanium alloys, Mater. Sci. Eng. A 260 (1999) 269–274.
[4] K. Miura, N. Yamada, S. Hanada, T.K. Jung, E. Itoi, The bone tissue compatibility of a new Ti-Nb-Sn alloy with a low Young's modulus, Acta Biomater. 7 (2011) 2020–2026.
[5] J. Coakley, K.M. Rahman, V.A. Vorontsov, M. Ohnuma, D. Dye, Effect of precipitation on mechanical properties in the β-Ti alloy Ti-24Nb-4Zr-8Sn, Mater. Sci. Eng. A 655 (2016) 399–407.
[6] D. Kuroda, M. Niinomi, M. Morigana, Y. Kato, T. Yashiro, Design and mechanical properties of new β-type titanium alloys for implant materials, Mater. Sci. Eng. A 243 (1998) 244–249.
[7] K. Wang, The use of titanium for medical applications in the USA, Mater. Sci. Eng. A 213 (1996) 134–137.
[8] X. Min, X. Chen, S. Emura, K. Tsuchiya, Mechanism of twinning-induced plasticity in β-type Ti–15Mo alloy, Scr. Mater. 69 (2013) 393–396.
[9] F. Sun, J.Y. Zhang, M. Marteleur, C. Brozek, E.F. Rauch, M. Veron, P. Vermaut, P.J. Jacques, F. Prima, A new titanium alloy with a combination of high strength, high strain hardening and improved ductility, Scr. Mater. 94 (2015) 17–20.
[10] M. Marteleur, F. Sun, T. Gloriant, P. Vermaut, P.J. Jacques, F. Prima, On the design of new β-metastable titanium alloys with improved work hardening rate thanks to simultaneous TRIP and TWIP effects, Scr. Mater. 66 (2012) 749–752.
[11] T. Saito, T. Furuta, J.-H. Hwang, S. Kuramoto, K. Nishino, N. Suzuki, R. Chen, A. Yamada, K. Ito, Y. Seno, T. Nonaka, H. Ikehata, N. Nagasako, C. Iwamoto, Y. Ikuhara, T. Sakuma, Multifuctional alloys obtained via a dislocation-free plastic deformation mechanism, Science 300 (2003) 464–467.
[12] Y. Yang, G.P. Li, G.M. Cheng, Y.L. Li, K. Yang, Multiple deformation mechanisms of Ti-22.4Nb-0.73Ta-2.0Zr-1.34O alloy, Appl. Phys. Lett. 94 (2009) 061901.
[13] R.J. Talling, R.J. Dashwood, M. Jackson, D. Dye, On the mechanism of superelasticity in Gum metal, Acta Mater. 57 (2009) 1188–1198.
[14] M. Tane, T. Nakano, S. Kuramoto, M. Niinomi, N. Takesue, H. Nakajima, Omega transformation in cold-worked Ti-Nb-Ta-Zr-O alloys with low body-centered cubic phase stability and its correlation with their elastic properties, Acta Mater. 61 (2013) 139–150.
[15] M. Besse, P. Castany, T. Gloriant, Mechanisms of deformation in gum metal TNTZ-O and TNTZ titanium alloys: a comparative study on the oxygen influence, Acta Mater. 59 (2011) 5982–5988.
[16] Y. Yang, S.Q. Wu, G.P. Li, Y.L. Li, Y.F. Lu, K. Yang, P. Ge, Evolution of deformation mechanisms of Ti-22.4Nb-0.73Ta-2Zr-1.34O alloy during strain, Acta Mater. 58 (2010) 2778–2787.
[17] E. Bertrand, P. Castany, I. Péron, T. Gloriant, Twinning system selection in a metastable β-titanium alloy by Schmid factor analysis, Scr. Mater. 64 (2011) 1110–1113.
[18] S. Hanada, O. Izumi, Deformation characteristics in β phase Ti-Nb alloys, Metall. Trans. A 11 (1985) 789–795.
[19] H.N. Han, C.S. Oh, G. Kim, O. Kwon, Design method for TRIP-aided multiphase steel based on a microstructure-based modelling for transformation-induced plasticity and mechanically induced martensitic transformation, Mater. Sci. Eng. A 499 (2009) 462–468.
[20] R. Ueji, N. Tsuchida, D. Terada, N. Tsuji, Y. Tanaka, A. Takemura, K. Kunishige, Tensile properties and twinning behavior of high manganese austenitic steel with fine-grained structure, Scr. Mater. 59 (2008) 963–966.
[21] H. Idrissi, K. Renard, D. Schryvers, P.J. Jacques, On the relationship between the twin internal structure and the work-hardening rate of TWIP steels, Scr. Mater. 63 (2010) 961–964.
[22] X.H. Min, K. Tsuzaki, S. Emura, K. Tsuchiya, Enhancement of uniform elongation in high strength Ti–Mo based alloys by combination of deformation modes, Mater. Sci. Eng. A 528 (2011) 4569–4578.
[23] D.L. Moffat, D.C. Larbalestier, The competition between martensite and omega in quenched Ti-Nb alloys, Metall. Trans. A 19 (1988) 1677–1686.
[24] S. Shin, C. Zhang, K.S. Vecchio, Phase stability dependence of deformation mode correlated mechanical properties and elastic properties in Ti-Nb gum metal, Mater. Sci. Eng. A 702 (2017) 173–183.
[25] Y. Guo, H. Abdolvand, T. Britton, A. Wilkinson, Growth of {1122} twins in titanium: a combined experimental and modelling investigation of the local state of deformation, Acta Mater. 126 (2017) 221–235.

[26] C. Zhu, V. Livescu, T. Harrington, O. Dippo, G.T. Gray III, K.S. Vecchio, Investigation of the shear response and geometrically necessary dislocation densities in shear localization in high-purity titanium, Int. J. Plast. 92 (2017) 148–163.
[27] W. Pantleon, Resolving the geometrically necessary dislocation content by conventional electron backscattering diffraction, Scr. Mater. 58 (11) (2008) 994–997.
[28] J. Jiang, T. Britton, A. Wilkinson, Evolution of dislocation density distributions in copper during tensile deformation, Acta Mater. 61 (19) (2013) 7227–7239.
[29] M.Y. Gutkin, T. Ishizaki, S. Kuramoto, I.A. Ovid'ko, N.V. Skiba, Giant faults in deformed gum metal, Int. J. Plast. 24 (2008) 1333–1359.
[30] M.Y. Gutkin, T. Ishizaki, S. Kuramoto, I.A. Ovid'ko, Nanodisturbances in deformed gum metal, Acta Mater. 54 (2006) 2489–2499.
[31] L. Wang, W. Lu, J. Qin, F. Zhang, D. Zhang, Microstructure and mechanical properties of cold-rolled TiNbTaZr biomedical β titanium alloy, Mater. Sci. Eng. A 490 (2008) 421–426.
[32] Y.L. Hao, M. Niinomi, D. Kuroda, K. Fukunaga, Y.L. Zhou, R. Yang, A. Suzuki, Young's modulus and mechanical properties of Ti-29Nb-13Ta-4.6Zr in relation to α″ martensite, Metall. Mater. Trans. A 33A (2002) 3137–3144.
[33] D.L. Moffat, D.C. Larbalestier, The competition between martensite and omega in quenched Ti-Nb alloys, Metall. Trans. A 19 (1988) 1677–1686.
[34] H.Y. Kim, Y. Ikehara, J.I. Kim, H. Hosoda, S. Miyazaki, Martensitic transformation, shape memory effect and superelasticity of Ti-Nb binary alloys, Acta Mater. 54 (2006) 2419–2429.
[35] Y. Ohmori, T. Ogo, K. Nakai, S. Kobayashi, Effects of ω-phase precipitation on β→α, α″ transformations in a metastable β titanium alloy, Mater. Sci. Eng. A 312 (2001) 182–188.
[36] Y. Mantani, Y. Takemoto, M. Hida, A. Sakakibara, M. Tajima, Phase transformation of α″ martensite structure by aging in Ti-8mass%Mo alloy, Mater. Trans. 5 (2004) 1629–1634.
[37] J. Coakley, K.M. Rahman, V.A. Vorontsov, M. Ohnuma, Effect of precipitation on mechanical properties in the β-Ti alloy Ti-24Nb-4Zr-8Sn, Mater. Sci. Eng. A 655 (2016) 399–407.
[38] X. Min, S. Emura, L. Zhang, K. Tsuzaki, K. Tsuchiya, Improvement of strength-ductility in β titanium alloy through pre-strain induced twins combined with brittle ω phase, Mater. Sci. Eng. A 646 (2015) 279–287.
[39] J.-L. Zhang, C.C. Tasan, M.J. Lai, D. Yan, D. Raabe, Partial recrystallization of gum metal to achieve enhanced strength and ductility, Acta Mater. 135 (2017) 400–410.
[40] X. Min, S. Emura, X. Chen, X. Zhou, K. Tsuzaki, K. Tsuzaki, K. Tsuchiya, Deformation microstructural evolution and strain hardening of differently oriented grains in twinning-induced plasticity β titanium alloy, Mater. Sci. Eng. A 659 (2016) 1–11.
[41] F. Sun, J.Y. Zhang, M. Marteleur, T. Gloriant, P. Vermaut, D. Laille, P. Castany, C. Curfs, P.J. Jacques, F. Prima, Investigation of early stage deformation mechanisms in a metastable β titanium alloy showing combined twinning induced plasticity and transformation-induced plasticity effects, Acta Mater. 61 (2013) 6406–6417.
[42] M.M. Wang, C.C. Tasan, D. Ponge, A.C. Dippel, D. Raabe, Nanolaminate transformation-induced plasticity-twinning-induced plasticity steel with dynamic strain partitioning and enhanced damage resistance, Acta Mater. 85 (2015) 216–228.
[43] M.M. Wang, C.C. Tasan, D. Ponge, D. Raabe, Spectral TRIP enables ductile 1.1 GPa martensite, Acta Mater. 111 (2016) 262–272.
[44] J.Y. Zhang, J.S. Li, Z. Chen, Q.K. Meng, F. Sun, B.L. Shen, Microstructural evolution of a ductile metastable β-titanium alloy with combined TRIP/TWIP effects, J. Alloy. Comd. 699 (2017) 775–782.
[45] S.R. Kalidindi, A.A. Salem, R.D. Doherty, Role of deformation twinning on strain hardening in cubic and hexagonal polycrystalline metals, Adv. Eng. Mater. 5 (2003) 229–232.
[46] A.A. Salem, S.R. Kalidindi, R.D. Doherty, S.L. Semiatin, Strain hardening due to deformation twinning in α-titanium: mechanisms, Metall. Mater. Trans. A 37A (2006) 259–268.
[47] J.H. Shen, Y.L. Li, Q. Wei, Statistic derivation of Taylor factors for polycrystalline metals with application to pure magnesium, Mater. Sci. Eng. A 582 (2013) 270–275.
[48] X.H. Min, K. Tsuzaki, S. Emura, T. Sawaguchi, S. Ii, K. Tsuchiya, {332} < 113 > twinning system selection in a β-type Ti-15Mo-5Zr polycrystalline alloy, Mater. Sci. Eng. A 579 (2013) 164–169.
[49] L. Jiang, J.J. Jonas, A.A. Luo, A.K. Sachdev, S. Godet, Twinning-induced softening in polycrystalline at moderate temperatures, Scr. Mater. 54 (2006) 771–775.
[50] T. Al-Samman, X. Li, S.G. Chowdhury, Orientation dependent slip and twinning during compression and tension of strongly textured magnesium AZ31 alloy, Mater. Sci. Eng. A 527 (2010) 3450–3463.
[51] L. Capolungo, P.E. Marshall, R.J. McCabe, I.J. Beyerlein, C.N. Tome, Nucleation and growth of twins in Zr: a statistical study, Acta Mater. 57 (2009) 6047–6056.
[52] J.J. Jonas, S. Mu, T. Al-Samman, G. Gottstein, L. Jiang, E. Martin, the role of strain accommodation during the variant selection of primary twins in magnesium, Acta Mater. 59 (2011) 2046–2056.
[53] M.R. Barnett, Z. Keshavarz, A.G. Beer, X. Ma, Non-Schmid behaviour during secondary twinning in a polycrystalline magnesium alloy, Acta Mater. 56 (2008) 5–15.
[54] M. Ashby, The deformation of plastically non-homogeneous materials, Philos. Mag. 21 (170) (1970) 399–424.